Chinese Journal of Mechanical Engineering

ORIGINAL ARTICLE

Open Access

Multi-Objective Optimization of VBHF in Deep Drawing Based on the Improved QO-Jaya Algorithm

Xiangyu Jiang[1,2], Zhaoxi Hong[1,2,3*], Yixiong Feng[1,2] and Jianrong Tan[1,2]

Abstract

Blank holder force (BHF) is a crucial parameter in deep drawing, having close relation with the forming quality of sheet metal. However, there are different BHFs maintaining the best forming effect in different stages of deep drawing. The variable blank holder force (VBHF) varying with the drawing stage can overcome this problem at an extent. The optimization of VBHF is to determine the optimal BHF in every deep drawing stage. In this paper, a new heuristic optimization algorithm named Jaya is introduced to solve the optimization efficiently. An improved "Quasi-oppositional" strategy is added to Jaya algorithm for improving population diversity. Meanwhile, an innovated stop criterion is added for better convergence. Firstly, the quality evaluation criteria for wrinkling and tearing are built. Secondly, the Kriging models are developed to approximate and quantify the relation between VBHF and forming defects under random sampling. Finally, the optimization models are established and solved by the improved QO-Jaya algorithm. A VBHF optimization example of component with complicated shape and thin wall is studied to prove the effectiveness of the improved Jaya algorithm. The optimization results are compared with that obtained by other algorithms based on the TOPSIS method.

Keywords Variable blank holder force, Multi-objective optimization, QO-Jaya algorithm, Algorithm stop criterion

1 Introduction

Deep drawing is a forming process that apply complex external force to the sheet through the punch, making the sheet material flow to the ideal direction. Refs. [1] and [2] review many parameters affecting the forming quality in the deep drawing process. For example, Zheng et al. [3] and Su et al. [4] studied the formability and performance of plates with different material properties. Modi et al. [5] and Srirat et al. [6] focused on the BHF to improve the forming quality. Lela et al. [7] determined the mathematical model of the friction coefficient in deep drawing. Karupannasamy et al. [8] and Gong et al. [9] explored influences of lubrication conditions on deep drawing process. Lin et al. [10] established the model related the tools shape parameters to the drawing stress-strain. Among these parameters, the BHF that the binder applies to the sheet is one of the most vital parameters. The friction resistance generated by the BHF can increase the tensile stress in the sheet, controlling the material flow. However, the BHF is a double-edged sword. An inappropriate BHF can result to forming defects. For example, a high BHF may cause sheet tearing, while a low BHF may cause sheet wrinkling. It is necessary to find a method that balance the BHF to maintain the best forming quality.

Compared with the BHF, the VBHF is an effective method that can significantly improve the forming quality. VBHF means the BHF varying differently in different

*Correspondence:
Zhaoxi Hong
hzhx@zju.edu.cn
[1] State Key Laboratory of Fluid Power and Mechatronic Systems, Zhejiang University, Hangzhou 310027, China
[2] Key Laboratory of Advanced Manufacturing Technology of Zhejiang Province, Zhejiang University, Hangzhou 310027, China
[3] Ningbo Innovation Center, Zhejiang University, Ningbo 315100, China

deep drawing steps. The VBHF can reduce or even eliminate the forming defects such as wrinkling, tearing and springback. The division of deep drawing steps are generally based on the shape of forming parts and material fluidity. Kitayama et al. [11–13] studied how to determine the VBHF trajectory. The VBHF trajectory has reference value for the experiment of determining the optimal VBHF value at an extent. However, the VBHF trajectories are not the same for deep drawing parts with different shapes. It is difficult to determine the appropriate VBHF only through continuous experiments. A high-efficiency optimization method based on advanced models and algorithms need be adopted.

The traditional optimization of the sheet deep drawing process is developed by the software simulation. Ablat et al. [14] took a review on numerical simulation of sheet metal forming. Kim and Hong [15] adopted finite element (FE) methods and Singh et al. [16] used LS-DYNA to optimize design of deep drawing process. Modi et al. [5] developed programmable logic controller and data acquisition system to determine the variable BHF path, predicting formability by FE simulations. A single simulation always costs a lot of time, even though the modern workstation. Meanwhile, after the samples collected, the establishment of optimization model is also a vital part. The methods based on mechanics theories have complex formula, various parameters and strict prerequisites. It had better be used as a mechanism analysis of forming defects rather than a large-scale solution. To improve the solution effectivity, the surrogate models are proposed to establish the mathematical expression of optimization. Manoochehri and Kolahan [17] and Tian et al. [18] adopted the artificial neural network (ANN) to build relation between process parameters and forming defects, Feng et al. [19] and Xie et al. [20] applied the Kriging model to replace time-consuming optimization solving by simulation test. Kitayama et al. [21–23] conducted sequential approximate optimization of process parameters with the radial basis function (RBF) model or the support vector machine (SVM) model. These models can approximate high-precision expression by fitting or interpolation with few samples. On the one hand, the surrogate models improve the optimization speed. On the other hand, the solution of surrogate models also needs high efficiency.

With the development of high-effective algorithms, more and more researchers combine the optimization algorithms with the mathematical simulation software and apply it in the solution of sheet deep drawing. The optimization algorithms mainly divide into deterministic and heuristic algorithms. Lin et al. [24] research that the deterministic algorithms (e.g., linear programming, dynamic programming and integer programming) obtain a global or an approximately global optimum by analyzing properties of the problem. Actually, the deterministic algorithms are not practical in engineering for it too complex to solve non-convex or large-scale optimization problems. Heuristic algorithms use the empirical rules to choose effective methods instead of seeking the answers systematically and in definite steps. It is more flexible, efficient and universal than deterministic algorithms, especially when the optimization problem is expressed in surrogate models. Choosing the heuristic algorithms as solver, the forming defects are set as optimization objectives and the VBHF as design variables. Algorithms solve objectives to find optimal design variables and the simulation software verifies whether the VBHF is excellent out of the simulation results. For instance, Manoochehri and Kolahan [17] employed simulated annealing algorithm to optimize the process parameters. Tian et al. [18] used ant colony algorithm, and Li and Wang [25] used differential evolutionary algorithm to solve VBHF. As the most popular algorithm in solving multi-objective problems, NSGA-II algorithm is applied in the VBHF optimization by Feng et al. [26].

According to summary of Rao [27], the population based heuristic algorithms include evolutionary algorithms (EA) and swarm intelligence (SI) algorithms. Almost all heuristic algorithms own common control parameters such as population size, iterations. Furthermore, different algorithms need their own specific control parameters. For instance, the specific control parameters of genetic algorithm are mutation probability, crossover probability, etc.; simulated annealing algorithm uses annealing start and end temperature, cooling speed, etc. These specific control parameters relate to the algorithm's performance significantly. The inappropriate adjustment of algorithm-specific parameters has the risk of increasing the solution time or falling into the local optimum. To avoid the risk brought by algorithm-specific parameters, Rao et al. [27, 28] introduced the teaching-learning-based optimization (TLBO) algorithm and the Jaya algorithm without any algorithm-specific parameters. They only need the common controlling parameters such as population size, generation number, random number. Compared with the TLBO algorithm's two-stage update, the Jaya algorithm just has one update stage. It solves optimization problems more simply with the similar precision. Therefore, we introduce the Jaya algorithm and improve it more suitable as the VBHF optimization solver in deep drawing.

After the comprehensive consideration, a new VBHF optimization method based on the improved Jaya algorithm is proposed. First, we focus on the VBHF

optimization of complex shape thin-walled parts. Tearing and wrinkling are the common defects of this type of parts. Thus, we choose tearing and wrinkling as multi-objectives. The evaluation criterions of wrinkling and tearing are established as constrains for limiting defects overlarge. Second, the BHF sample points are selected by Latin Hypercube Sampling (LHS). The Kriging model have advantages of good adaptability, smoothness and minimum estimation variance. We use Kriging surrogate model to approximate the mathematical relation between the VBHF and two defects. Third, we adopt the Jaya algorithm as optimization solver. The Jaya algorithm is added quasi-oppositional strategy and innovated stop criterion for enhancing the convergence speed. Finally, the method we proposed is applied in a case study of complex shape thin-walled parts. The Pareto solution are scored and sorted by decision algorithm TOPSIS. The improved Jaya algorithm are compared with the original Jaya algorithm and NSGA-II algorithm, which prove the efficiency of the QO-Jaya algorithm. The main contributions of this paper are as follows.

1) The optimization model considering wrinkling and tearing is established by LHS and Kriging surrogate method. The operation is solved by a novel algorithm named Jaya that is unique in without algorithm-specific parameters and only having common control parameters, thus superior in saving solution times and universality of the algorithm.
2) "Quasi-oppositional" strategy is added to Jaya algorithm for improving population diversity. The strategy of opposition based learning is used to generate a population opposite to the current population. It further diversifies the population and accelerates the convergence rate of Jaya algorithm.
3) To ensure the optimization process converges reasonably, a stop criterion based on the "*spread*" measurement for each iteration is proposed to evaluate the Jaya algorithm optimization situation. The measurement index "*spread*" is defined to reflect the convergence of the solutions objectively.

The rest of the paper is organized as follow: In Section 2, the evaluation criteria of tearing and wrinkling are put forward and the optimization problem is described preliminary. In Section 3, the Kriging surrogate model provide optimization problem the mathematical expression, including objectives and constrains. Section 4 introduces the improved QO-Jaya algorithm and the improvement scheme. Section 5 is a case study about VBHF optimization on a complex shape thin-wall part. The conclusion and future research are presented in Section 6.

2 Defect Evaluation Criteria and VHBF Optimization Problem Framework

The main defects in deep drawing process are the wrinkling of the flange, and the tearing at the tangent of the bottom fillet and the straight wall. Wrinkling can be solved by applying BHF. However, with the increase of BHF, tearing at the tangent of the bottom fillet and straight wall are likely to occur. Generally, the wrinkling and tearing are considered at the same time in practical applications.

2.1 Tearing Assessment

The tearing of sheet is related to material strength limit. The tensile stress exceeds the strength limit of the material during the deep drawing. The dangerous section of the drawing part is where the lower end of the cylinder wall meets the outer corner. The excessive strain at the dangerous section causes the wall thickness excessively thin, which leads to tearing.

The degree of tearing can be reflected by the maximum thinning rate. Shown in the study by Feng et al. [19, 26], the maximum thinning rate is defined as follows:

$$\eta_{\max}=\frac{t_0-t_{\min}}{t_0}\times 100\%, \tag{1}$$

where $\eta_{\max}$ is the maximum thinning rate, t_0 is the initial sheet thickness, and $t_{\min}$ is the thinnest sheet thickness of the thin-walled member after deep drawing. In order to prevent tearing during the deep drawing process, it is usually stipulated that the maximum thinning rate shall not exceed the critical value. Therefore, the evaluation criterion of tearing is

$$\eta_{\max}\leq\eta_{cr}, \tag{2}$$

where η_{cr} is the critical thinning rate. It usually set as 25% according to experience. The maximum thinning rate has been widely used in actual production for its intuition and easy understanding.

2.2 Wrinkling Assessment

Wrinkling is a major harmful phenomenon in the deep drawing process. Slight wrinkling affects the forming accuracy and surface smoothness of parts. Severe wrinkling prevents the sheet material from flowing into the gap between the punch and die, resulting in the sheet tearing and become waste. Wrinkling is a phenomenon of plastic deformation instability. There are three reasons for wrinkling: the pressure bar instability caused by the pressure stress, the uneven stress in the deformation zone, and the shear stress effect. Flange wrinkling and sidewall wrinkling are two forms of wrinkling. Flange wrinkling usually reaches the maximum in the

initial stage of deep drawing. Sidewall wrinkling is usually accompanied by flange wrinkles. Thus, the flange part is mainly considered in the calculation of the critical wrinkling BHF.

The evaluation indicators of wrinkling are the maximum thickness strain and the wrinkling height. The maximum thickness strain can reflect the wrinkling trend of the sheet during the deep drawing process, and the wrinkling height reflects the wrinkling severity of the drawn part truly during deep drawing.

When the sheet is wrinkled, the distance L between the die and the blank is greater than the initial thickness t_0. Therefore, the wrinkle evaluation criterion can be expressed by the distance between the die and the blank

$$L > B \times t_0, \tag{3}$$

where L is the distance between the die and the blank, t_0 is the initial thickness of thin-walled components, B is a safety factor. According to engineering experience, B always takes 1.2.

Springback is another common forming defect in addition to wrinkling and tearing. In this paper, we omitted the consideration of springback because it seldom appears in the complex shape thin-wall part.

2.3 Model of the VHBF Optimization Problem

The optimization of VBHF includes the determination of design variables, objectives and constraints. The design variables are BHFs in different deep drawing stage, that is, in the different punch stroke. In Figure 1, the total punch stroke is partitioned into n steps $S = [S_1, S_2, \ldots, S_n]$. Correspondingly, the BHFs takes n different values $F_{VBH} = [F_{VBH_1}, F_{VBH_2}, \ldots, F_{VBH_n}]$. Every F_{VBH} is a design variable in the optimization. The divided steps are not changeless. It is mainly determined by the characteristics of the hydraulic press itself and the drawing parts shape.

After the VBHF curve established, the objectives and constrains can be determined. The objectives are that minimize the evaluation of tearing and wrinkling. There are three constrains. One is the range of BHF, and another are the evaluation of wrinkling and tearing that not exceed the limitation settled in Section 2.1 and Section 2.2. The description of optimization problem is as follows:

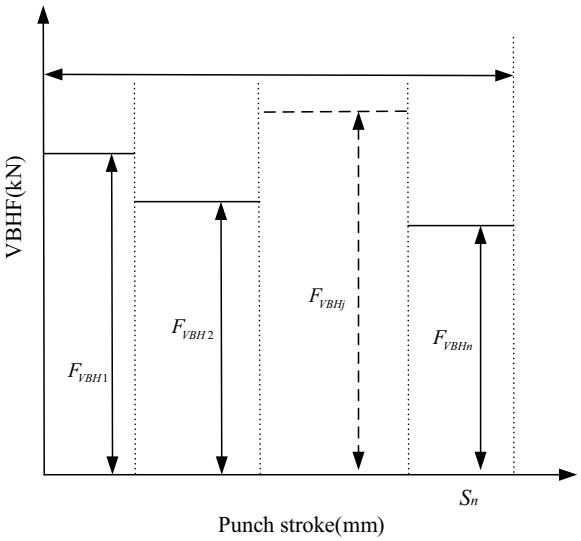

Figure 1 The step partition of the punch stroke and the VBHF

$$\begin{cases} \min f_1(F_{VBH}) = \eta_{\max}, \\ \min f_2(F_{VBH}) = L, \\ \text{s.t.,} \quad F_{VBH}^L \le F_{VBHj} \le F_{VBH}^H, \quad j = 1, 2, ..., n, \\ L < B \times t_0, \\ \eta_{\max} \le \eta_{cr}. \end{cases} \tag{4}$$

After the model of optimization problem built initially, the specific expression of problem is needed for solving. There are two main methods to build a solution model. One is the method based on the software simulation, that is, use finite element analysis model to select BHF and experiment continuously. The other one is using the surrogate model to approximate the evaluation of tearing and wrinkling. The simulation is time-consuming and requires high computer hardware. However, it is easier to use surrogate model and the accuracy of the surrogate model is guaranteed. In this paper, the Kriging surrogate model is selected for modeling. The simulation software, Dynaform, is applied to verify the effectiveness of the optimums.

3 Mathematical Expression Based on Kriging Model for VBHF Optimization in Deep Drawing

3.1 Introduction of Kriging Surrogate Model

The Kriging surrogate model has the characteristics of smoothness and minimum estimation variance. It can fit problems with high nonlinearity ideally. It is widely used to fit low-order or high-order nonlinear problems, concluded by study of Zhao et al. [29]. The Kriging surrogate model is essentially an interpolation method

based on statistical theory. Its basic principle is to construct an approximate model of the objectives through known samples and their responses. And then use the constructed model to predict unknown samples and their responses. The Kriging surrogate model consists of a global model and a local random deviation function, that is, a combination of a parametric model and a non-parametric random process. The Kriging surrogate model is more flexible than a single parametric model. And it also overcomes the limitation of non-parametric models in processing high-dimensional data.

The expression form of Kriging surrogate model is

$$\tilde{y}(x) = F\beta + z(x), \tag{5}$$

where $F = [f_1(s_1), f_2(s_2), ..., f_q(s_m)]^{\mathrm{T}}$ is a known regression model, generally a polynomial model, including polynomials of zero-order, first-order, second-order and so on; $\beta = [\beta_1, \beta_2, ..., \beta_q]^{\mathrm{T}}$ is the corresponding regression coefficients to be estimated; $z(x)$ is a stationary stochastic process, and $E[z(s)]$=0, $\mathrm{cov}(z(s), z(x)) = \sigma^2 \tilde{R}(\theta, s, x)$. $\tilde{R}(\theta, s, x)$ is a correlation function about parameter θ, which generally takes Gaussian correlation function

$$\tilde{R}(\theta, s, x) = \prod_{i=1}^{n} \exp(-\theta |s_j - x_j|^2). \tag{6}$$

$F\beta$ provides a global approximation of the Kriging model and $z(x)$ provides an approximation of the local variation of the model. Kriging surrogate model is used to realize the nonlinear fitting between the input data (VBHF) and the output data (the response value of each VBHF). In Section 3.2, the VBHF optimization model constructed by Kriging method will be introduced in detail.

3.2 Kriging Surrogate Model of VBHF Optimization

In this section, the optimal Latin Hypercube Design (LHD) will be used to select sample points. The Kriging model will be constructed based on these sample points. Then the relationship will be established between VBHF and forming defects in the deep drawing process. The whole steps of establishing and solving the VBHF optimization problem is shown in Figure 2.

McKey et al. [30] proposed the Latin Hypercube Design (LHD). The LHD have been widely used in sampling in various large-scale design spaces. In the VBHF optimization, the sample array $\{(V_1, Y_1)...(V_i, Y_i)...(V_k, Y_k)\}$ can be obtained by LHD, where k is the number of samples, V_i $(i = 1,2,...,k)$ is the ith sample point in VBHF design space, and Y_i is the response corresponding to the sample V_i obtained by the Dynaform simulation software.

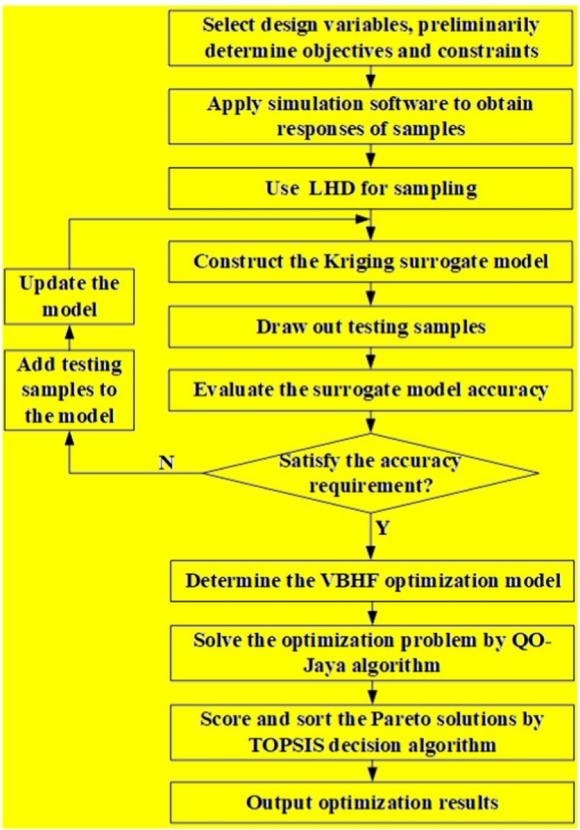

Figure 2 Framework of VBHF optimization using proposed method in deep drawing

In view of the fact that the sample points taken in the symmetric LHD are more uniform, it is also more conducive to the establishment of subsequent approximation models. In this paper, the symmetric LHD is used for the adoption of the design space. Considering the 6-dimensional design space is hard for visualization, we take a 2-dimensional design space to extract 30 sample points as an example to illustrate the symmetric LHD sampling scheme, as shown in Figure 3.

Based on the VBHF optimization model represented by Eq. (4), we convert the objectives and constrains with solvable mathematical form. The approximate models of wrinkling and tearing are constructed based on Kriging surrogate model, as follows:

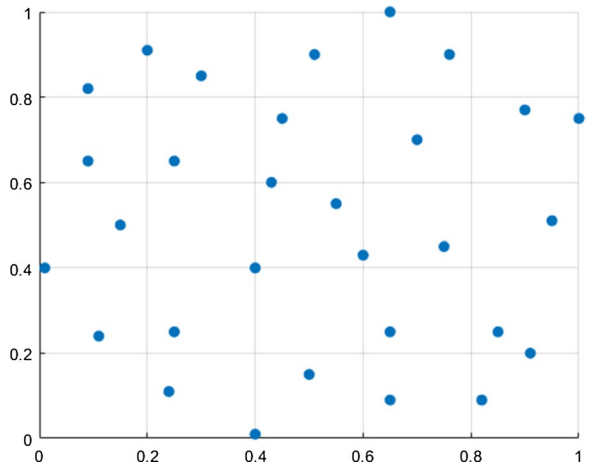

Figure 3 The symmetric LHD (30 sampling points)

$$\begin{cases} \min \tilde{f}_W(F_{VBH}), \tilde{f}_T(F_{VBH}), \\ \tilde{f}_W(F_{VBH}) = \beta_W F_W(F_{VBH}) + z_W(F_{VBH}), \\ \tilde{f}_T(F_{VBH}) = \beta_T F_T(F_{VBH}) + z_T(F_{VBH}), \\ \text{s.t.}, \tilde{f}_W(F_{VBH}) < B \times t_0, \\ \tilde{f}_T(F_{VBH}) < \eta_{cr}, \\ F_{VBH}^L \le F_{VBH} \le F_{VBH}^H, \\ F_{VBH} = (F_{VBH1}, \ldots F_{VBHj}, \ldots F_{VBHn})^{\mathrm{T}}, \end{cases} \tag{7}$$

where $\tilde{f}_W(F_{VBH})$ and $\tilde{f}_T(F_{VBH})$ are the approximate expresses of wrinkling and tearing respectively, $\beta_W F_W(F_{VBH})$ and $\beta_T F_T(F_{VBH})$ are the regression models of wrinkling and tearing respectively, $z_W(F_{VBH})$ and $z_T(F_{VBH})$ are the random deviation in the regression models of wrinkling and tearing respectively.

4 Multi-objective Quasi-oppositional Based Jaya Algorithm

Jaya algorithm is a relatively new swarm intelligence algorithm, which was proposed first by Rao [27] in 2016. The optimization principle of Jaya algorithm is that the solution should move towards the best solution but avoid the worst one. The most significant feature of Jaya algorithm is which only has common control parameters without algorithm-specific control parameters. This feature makes the algorithm more easily in initial parameters setup, thereby reducing the time cost and ensuring the stable performance. Rao et al. [31] and Zhang et al. [32] proved the effectiveness of algorithm through solving various constrained and unconstrained engineering optimization problems or benchmark problems. And the computational results reveal that the Jaya algorithm is superior to or comparable with other optimization algorithms.

After the Jaya algorithm presenting, there have been various improvement and strategies added in it for better performance. In order to handle multiple objectives simultaneously, Rao et al. [33] proposed the multi-objective Jaya (MO-Jaya) algorithm. Some changes are aimed to further diversify the population and increase the convergence speed of the Jaya algorithm. For example, Rao and More [34] proposed the self-adaptive Jaya algorithm that determined the population size automatically to improve the population diversity; Rao and Rai [35] advanced the quasi-oppositional based Jaya algorithm, which generated a population opposite to the current population to keep the randomness of Jaya algorithm. Meanwhile, it is also important for algorithm to balance the global exploration and local exploitation. In researches of Farah and Belazi [36] and Yu et al. [37], the chaotic Jaya algorithm use the chaotic sequence generated by the chaotic graph rather than random numbers to balance the exploration and exploitation. Rao and Saroj [38] added the elitist stratagem in Jaya algorithm. It replaces the worst solution(s) with the elitist one(s) to effectively control Jaya algorithm for the transition from global exploration to local exploitation. Besides, there are some other tiny improvements, such as adopting a neighborhood search strategy to enhance the population diversity, linearly decreasing inertia weights to enhance development efficiency, or a combination of the above strategies. The summary of the improvement strategies on Jaya algorithm is shown in Figure 4, which is divided according to the specific improvement objects.

Nowadays, the Jaya algorithm is applied in continuous/discrete, high-dimensional/low-dimensional, or linearity/nonlinearity optimization problems. The professional fields of application include electronic and electrical engineering, energy engineering, mechanical engineering, management science, computer science and so on. It has not been applied to drawing forming process optimization yet. In this paper, we will first use

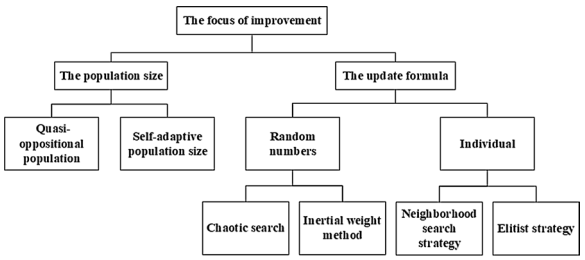

Figure 4 Summary of the improvement strategies on Jaya algorithm

Jaya algorithm to solve the VBHF optimization of sheet in deep drawing.

4.1 Introduction of the Multi-objectives Jaya Algorithm

Like the common heuristic algorithm, Jaya algorithm has the common control parameters such as the population size, generation number, etc. The initial population is generated randomly within the ranges of variables. However, it is different from other heuristic algorithms that Jaya algorithm only have one update function. It is more quickly in updating population. In every generation, the population updates based on Eq. (8):

$$\begin{aligned} W'_{g,p,j} &= W_{g,p,j} + r_{1,g,j}(W_{g,best,j} - |W_{g,p,j}|) \\ &\quad - r_{2,g,j}(W_{g,worst,j} - |W_{g,p,j}|), \\ g &= 1,2,\ldots,G; p = 1,2,\ldots,Pop; j = 1,2,\ldots,n, \end{aligned} \tag{8}$$

where G is the max generation number; g means the gth generation. Pop is the population size; p means the pth individual. n is the number of variables; j means the jth variable. In Eq. (7), $W'_{g,p,j}$ is the updated new individual, $W_{g,p,j}$ is the old individual, $r_{1,g,j}$ and $r_{2,g,j}$ are the random number in [0,1]. $W_{g,best,j}$ and $W_{g,worst,j}$ are respectively the best and worst solutions in the gth generation, the jth variable. $(W_{g,best,j} - |W_{g,p,j}|)$ means the tendency of the solution towards the best solution, while $(W_{g,worst,j} - |W_{g,p,j}|)$ means the tendency of the solution far from the worst solution. In the function, the random number act as scaling factor to ensure good exploration performance. The best and worst solutions guarantee the positive direction of the update solution. At the end of the iteration, all acceptable solutions will be retained and become the inputs for the next generation.

Since the VBHF optimization we researched is a multi-objective problem, the Jaya algorithm needs some strategies added to convert to the multi-objectives Jaya algorithm. In the multi-objectives Jaya algorithm, the concepts of constraint-dominance sorting, non-dominance sorting and crowding distance computation are used to determine the rank of solutions. These principles are the keys for conducting the searches of Pareto frontier. The sorting principles are explained by Figure 5. The flowchart of the multi-objectives Jaya algorithm is shown in Figure 6.

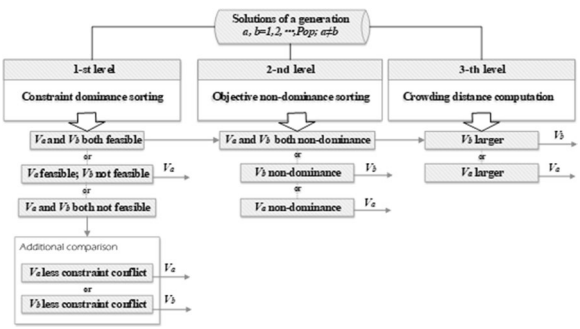

Figure 5 The sorting principles of constraint-dominance sorting, non-dominance sorting and crowding distance computation

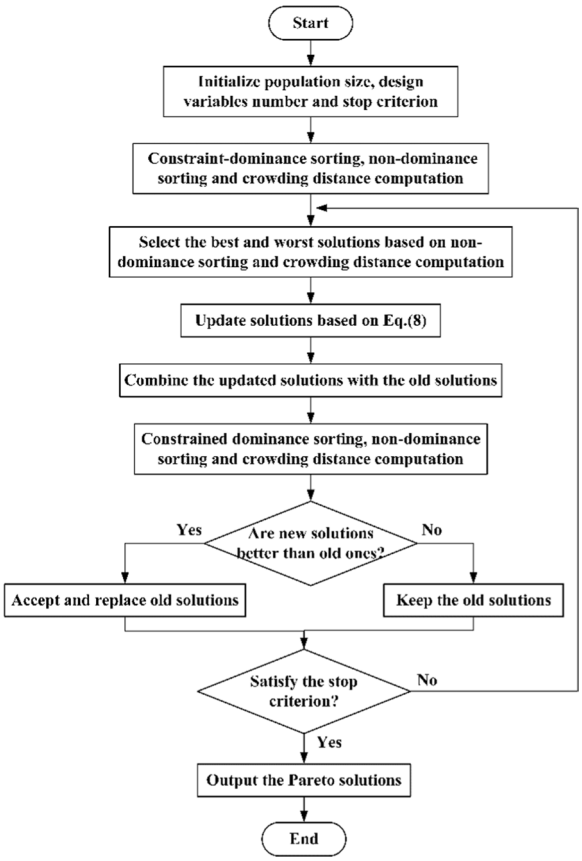

Figure 6 Flowchart of the multi-objectives Jaya algorithm

The detailed solving steps of multi-objective Jaya algorithm is described as follows.

Step 1: *Pop* solutions are generated randomly as an initial population. The initial population is sorted based on the principles of constraint-dominance and non-dominance.

Step 2: First, the constraint-dominance is used to determine the superiority between solutions initially. Then the non-dominance and crowding distance are conducted to further determine the priority of the solution. The solution with a higher rank is better than the other one. If the solutions have the same rank, the solution with a higher crowding distance is considered better than the other one.

Step 3: Choose the solution with the highest rank (rank = 1) as the best solution and the solution with the lowest rank is the worst solution. Then the solution of next generation can be updated according to Eq. (7).

Step 4: After the solutions updated, the new solutions combine with the old solution as 2*Pop* solutions. Reorder these solutions according to the principles of constraint-dominance, non-dominance sorting and crowding distance computation. Then select *Pop* solutions as the new population based on the new sorting.

Step 5: Turn to Step 3 to update generation until satisfy the stop criterion.

The concept of constraint dominance guarantees that feasible solutions have a higher rank than infeasible solutions. Among the feasible solutions, the superior solution (non-dominated solution) ranks higher than the dominated solution. Among the infeasible solutions, a higher rank is assigned to the solution with less overall constraint conflict. The use of crowding distance for non-dominated sorting ensures that the solution is selected from the sparse area of the search space.

4.2 Introduction of the Multi-objectives Jaya Algorithm

4.2.1 Quasi-oppositional Based Strategy

QO-Jaya algorithm means Quasi-oppositional based Jaya algorithm, which is added a concept of opposition based learning in common Jaya algorithm. A population opposite to the current population is generated to further diversify the population and accelerate the convergence rate of Jaya algorithm. We improve the quasi-oppositional population generation strategy for better practicality in programming. The opposite population is generate based on Eqs. (9)–(11):

$$a = \frac{W_j^L + W_j^U}{2}, \tag{9}$$

$$b = W_j^L + W_j^U - W_{g,p,j}, \tag{10}$$

$$W_{g,p,j}^q = a + (b - a) * r_3, \tag{11}$$

where W_j^L and W_j^U are the lower and upper bounds of the variables range. $W_{g,p,j}$ is the current population and $W_{g,p,j}^q$ is the opposite population to the current population. r_3 is the random number in [0, 1]. a means the midpoint of the variables interval and b means the mirror point of the variables.

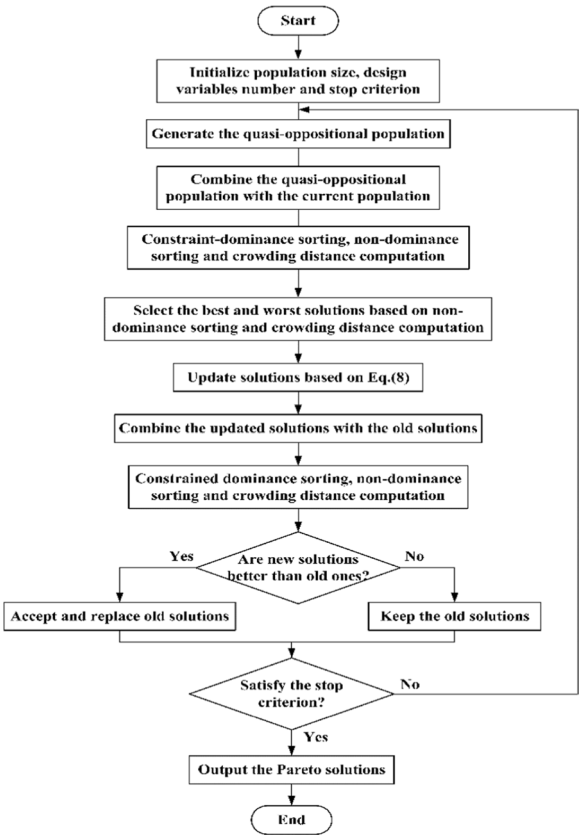

Figure 7 Flowchart of the improved QO-Jaya algorithm

4.2.2 Improved Stop Criterion

In most optimization algorithm, the stop criterion is usually the generation number reaches a max generation number or the cumulative individuals reach the limitation. Both the stop criteria are set rigidly by cumulative sum of counting parameters without reflecting the solutions condition. In this case, some solving progress that solutions have converged may continue searching meaninglessly. This greatly reduces the solution speed and waste resources on unnecessary computation.

In this paper, a measurement index '*spread*' is defined to reflect the solutions convergence objectively. We propose a stop criterion based on *spread*: when the *spread* does not change much, the *spread* of current generation is smaller than the average of previous *spread*, and this condition is maintained for a certain number of times, the algorithm will stop. The *spread* is calculated by Eq. (12). We set the population size to 50, 100, and 500 for testing, which proves the stop criterion effective.

$$Spread = \frac{\mu + \sigma}{\mu + k \cdot \sigma}, \tag{12}$$

$$\mu = \left\| \tilde{f}_W(W_{g,best}) - \tilde{f}_W(W_{g-1,best}) \right\| + \left\| \tilde{f}_T(W_{g,best}) - \tilde{f}_T(W_{g-1,best}) \right\|, \tag{13}$$

where k is the number of objective functions, σ is the standard deviation of the crowding distance measure of points that are on Pareto front with finite distance. μ is the norm of the difference between the minimum objective on the Pareto front of the current generation and that of the previous generation. As there are two objectives in this study, μ is the sum over the two norms of objective functions shown as Eq. (13). $W_{g,best}$ and $W_{g-1,best}$ indicate the parameters for the minimum objective on the Pareto front of the current generation and the previous generation, respectively.

The *spread*-based stop criterion can make the convergence measurement of the design variables more objective, for it is not affected by parameters other than the number of iterations. The *spread* not only reflects the change of the congestion degree of the Pareto front, but also reflects the movement of the Pareto front. It is also found from experiment that many Pareto fronts may jump and escape from the best solution obtained before after satisfying the stop criterion once. This indicates that the Pareto front is not stable finally yet. Therefore, in order to maintain more stable and reliable Pareto optimal solutions, the algorithm will finally stop after reaching the stop criterion 5 times. Write the program in the algorithm to count the total number of the times that accumulatively satisfying the stop criterion. The flowchart of the improved QO-Jaya algorithm is shown in Figure 7.

5 Case Study

The complex outer shell thin-walled parts have many sharp inflection points. It is easy to cause wrinkling, tearing and other problems in the deep drawing process. Figure 8 shows the complex outer shell thin-walled parts that we optimized in case study. In this section, we conduct the VBHF optimization of a specific complex outer thin-walled parts.

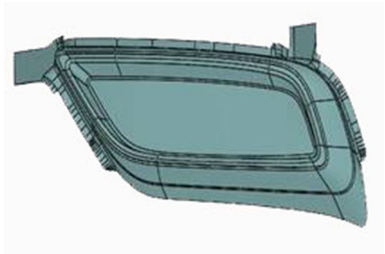

Figure 8 The complex outer shell thin-walled parts

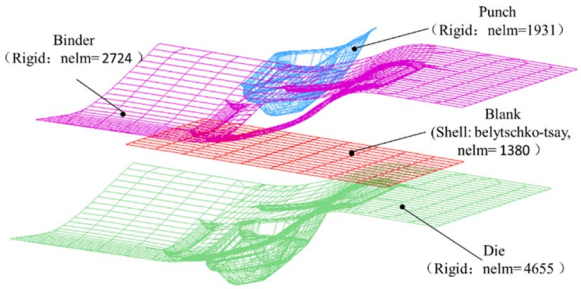

Figure 9 Simulation analysis model of the complex outer shell thin-walled part

5.1 Parameters of the Complex Outer Shell Thin-walled Part

The material is 304L stainless steel. The simulation analysis model of the complex outer shell thin-walled part is shown in Figure 9.

The entire drawing stroke is divided into 6 phases, each phase adopts a different BHF. According to experience, the range of each BHF is [500 kN, 2000 kN], taking wrinkling and tearing as objectives. The constrains are all set

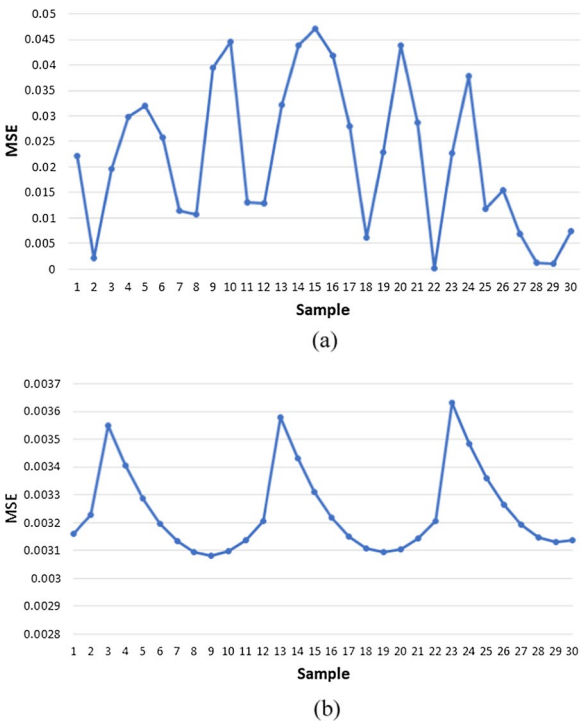

Figure 10 The mean square error of Kriging model: (**a**) The error of tearing objective function, (**b**) The error of wrinkling objective function

by experience. The multi-objective optimization model of VBHF is established as follows:

5.2 VBHF Optimization Solution of Complex Outer Shell Thin-walled Part in Deep Drawing

After the simulation model conducted, the LHD is used to sample the initial BHF and defects measurements of the sheet in deep drawing. Sampling is performed in 6-dimensional space and 30 sample points are collected. Then establish the Kriging surrogate model of objectives $\{\tilde{f}_W(F_{VBH}),\tilde{f}_T(F_{VBH})\}$ based on the samples. The expression of the model is as follows:

- Tearing objective function

$$\begin{aligned}\tilde{f}_T(F_{VBH}) =& 5.7858\times10^{-7}+0.0180F_{VBH1}\\&-0.2837F_{VBH2}+0.0739F_{VBH3}\\&+0.2315F_{VBH4}-0.1374F_{VBH5}\\&-0.0805F_{VBH6}+r(\theta,d)\gamma.\end{aligned}\tag{14}$$

- Tearing objective function

$$\begin{aligned}\tilde{f}_W(F_{VBH}) =& 6.8894\times10^{-6}-0.1456F_{VBH1}\\&+0.2251F_{VBH2}+0.0214F_{VBH3}\\&-0.0047F_{VBH4}+0.0761F_{VBH5}\\&-0.0365F_{VBH6}+r(\theta,d)\gamma.\end{aligned}\tag{15}$$

The kriging model is the best unbiased estimate based on the interpolation method. It completely passes through the sample points. Figure 10 shows the mean square error of Kriging model.

The improved QO-Jaya algorithm is used to solve the established optimization model. Set the max individual number as 37500, and the population size is 100. The 100 initialized individuals.

5.2.1 Iteration Process

After initializing the 100 individuals of a population, generate the quasi-opposition population of the initialized population. Combine the two populations to sort and selected the first 100 individuals as a new population. Then update the current population, sort the new and old individuals to the best 100 individuals. Update the quasi-opposition population and repeat the iteration as before.

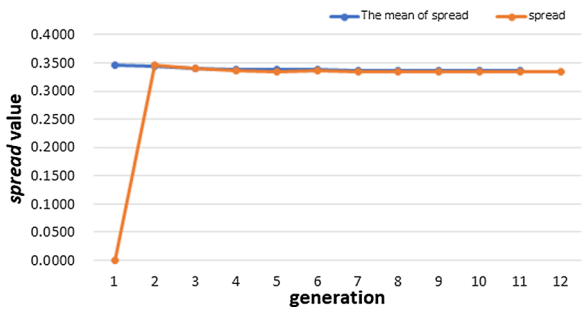

Figure 11 The comparison between *spread* and the mean of *spread*

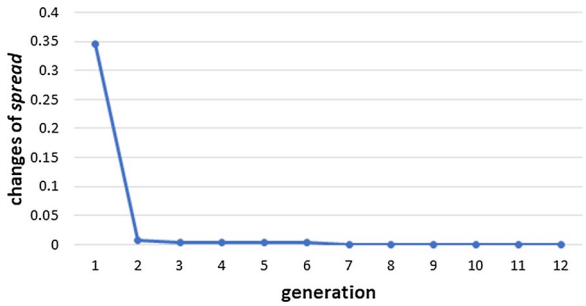

Figure 12 The changes of *spread*

5.2.2 Convergence Process

The *spread* measures whether the Pareto solutions have converged effectively. The final convergence results are as follows:

The algorithm runs for 12 generations, and the *spread* order of each generation is: 0, 0.3465, 0.3400, 0.3360, 0.3334, 0.3366, 0.3334, 0.3333, 0.3333, 0.3334, 0.3333, 0.3333. The mean of *spread* in 12 generation are 0.3465, 0.3432, 0.3408, 0.3390, 0.3385, 0.3376, 0.3370, 0.3366, 0.3362, 0.3359, 0.3357, respectively. Figure 11 shows the comparison between *spread* and the mean of *spread*. The order of changes in *spread* is 0.3465, 0.0065, 0.0040, 0.0026, 0.0032, 0.0032, 3.9357×10^{-5}, 2.1998×10^{-5}, 2.1998×10^{-5}, 7.8417×10^{-6}. It can be seen from Figure 12 that the change of *spread* decreases rapidly and stabilizes gradually. Both of the evaluating indicators maintain the effective convergence of solutions.

The algorithm will stop when the principle satisfied in 5 times. The principle is that the *spread* has not changed much and the final *spread* is less than the average of the most recent *spread*s.

5.2.3 Optimization Results

The solutions are scored and sorted by the decision algorithm TOPSIS. The solution with highest score is shown in Table 1. It can be seen that the risk of wrinkling has reduced 5.1% and that of tearing has reduced 42.6%. It can be concluded that the VBHF optimization improves the forming quality of complex outer shell thin-walled part in deep drawing process. For better representation of the optimization effect, we use Dynaform to simulate the optimized VBHF, as shown in Figures 13, 14.

Table 1 Comparison between the original constant BHF and the optimized VBHF

	F_{VBH1} (kN)	F_{VBH2} (kN)	F_{VBH3} (kN)	F_{VBH4} (kN)	F_{VBH5} (kN)	F_{VBH6} (kN)	Wrinkling L (mm)	Tearing η_{max} (%)
The original parameters	1000	1000	1000	1000	1000	1000	1.157	24.768
The optimized parameters	1168.948	1728.490	731.1526	1088.581	1567.474	1895.709	1.098	14.210

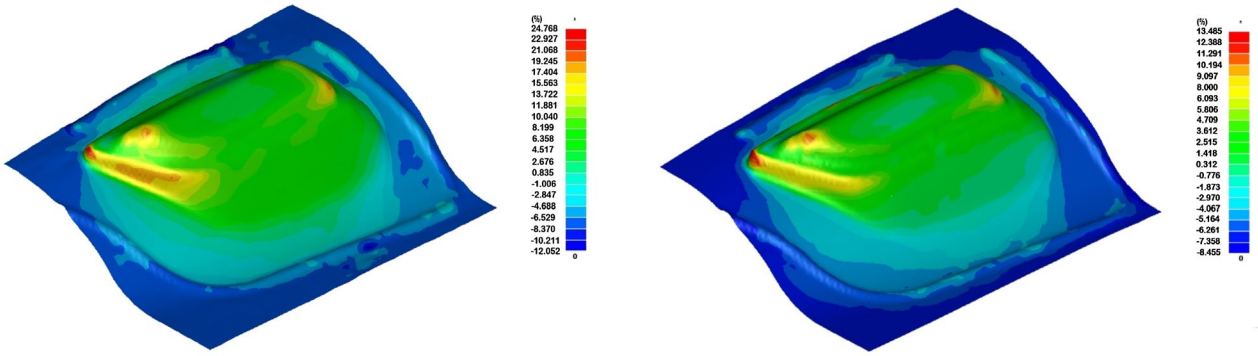

Figure 13 The comparison of tearing between complex outer liner thin-walled parts before and after optimization: (**a**) Before optimization, (**b**) After optimization

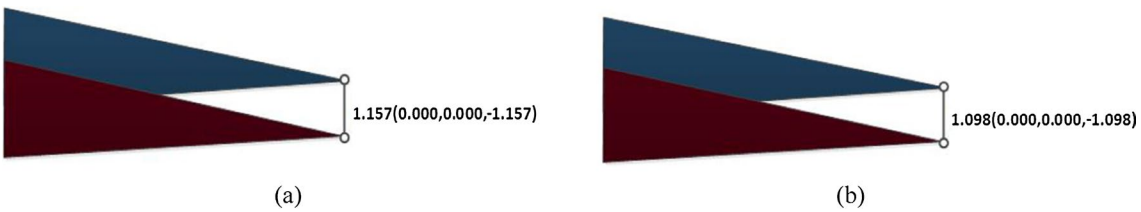

Figure 14 The comparison of wrinkling between complex outer liner thin-walled parts before and after optimization: (**a**) Before optimization, (**b**) After optimization

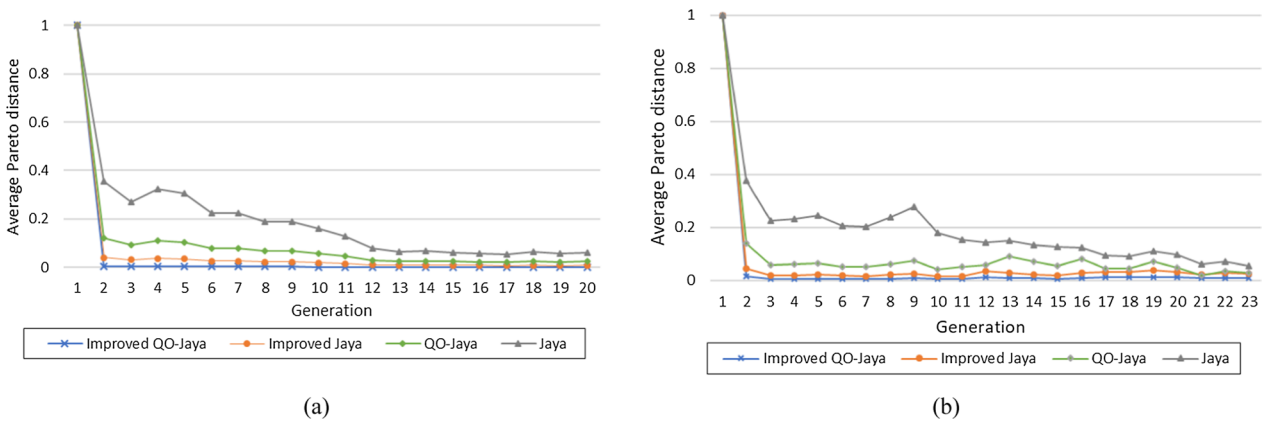

Figure 15 The comparison of iteration curves between QO-Jaya algorithm (improved or not) and Jaya algorithm (improved or not): (**a**) 500 population size, (**b**) 50 population size

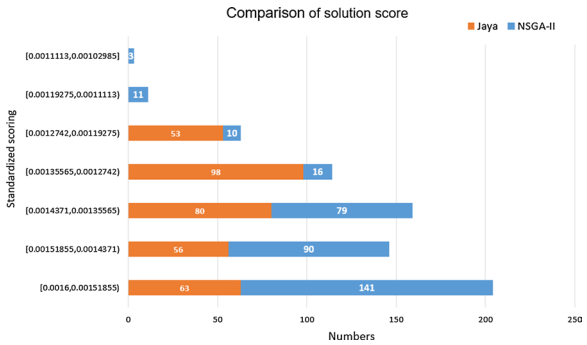

Figure 16 Comparison of solution scores between QO-Jaya algorithm and the NSGA-II algorithm

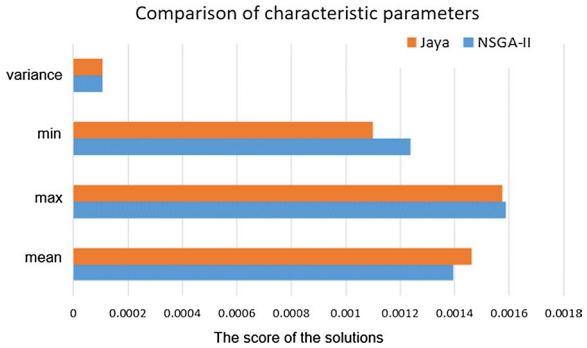

Figure 17 Comparison of characteristic parameters of QO-Jaya algorithm and the NSGA-II algorithm

5.3 Discussion and Comparison

In this section, the improved QO-Jaya algorithm is compared with the common QO-Jaya algorithm, the Jaya algorithm added stop criterion, the common Jaya algorithm and NSGA-II algorithm. The comparison with the first three kinds of Jaya algorithm is to explain the advantages of improved strategies. The comparison with NSGA-II algorithm is to show the effectives of QO-Jaya algorithm in solving problem.

The comparison with the first three kinds of Jaya algorithm is shown in Figure 15. When the population size is 50, QO-Jaya algorithm runs for 20 generations, and Jaya algorithm runs for 22 generations. The improved QO-Jaya algorithm runs for 9 generations, and improved Jaya algorithm runs for 12 generations. When the population size is 500, QO-Jaya algorithm runs for 13 generations, and Jaya algorithm runs for 14 generations. The improved QO-Jaya algorithm runs for 9 generations, and improved Jaya algorithm runs for 12 generations. In general, the Jaya algorithms without improved strategies are waste more time on meaninglessly searching. And the improved Jaya algorithms are convergent faster. However, the QO-Jaya algorithm is superior to the Jaya algorithm no matter having improved strategies or not. Sorted by the TOPSIS algorithm, the solutions of improved QO-Jaya algorithm are at a higher ranking.

The next is the comparison between QO-Jaya algorithm and NSGA-II. After comparing the scatter plots of design variables, QO-Jaya algorithm is better than NSGA-II algorithm in the dispersion degree of solutions. QO-Jaya algorithm can obtain boundary points. Many solutions generated by NSGA-II algorithm are concentrated near the boundary but cannot be obtained the boundary value. After sorting by TOPSIS, the solution is divided into 7 intervals spaced equally (shown in Figure 16). QO-Jaya algorithm has solutions in the first 5 intervals, and the number of each intervals is not very different. The solutions generated by NSGA-II algorithm are distributed on all the 7 intervals, and the individuals number decreases gradually as the score decreases. The number is also gradually decreasing. The mean and variance of the two algorithms are not much different (shown in Figure 17). However, the continuous optimal individuals in the ranking are generated by QO-Jaya algorithm, and the continuous worst individuals are generated by the NSGA-II algorithm. It is confirmed that QO-Jaya algorithm presents the good solving performance.

6 Conclusions

In this paper, we propose a VBHF optimization method based on the improved QO-Jaya algorithm for the complex outer shell thin-walled part in deep drawing. The VBHF optimization is conducted to reduce the risk of forming defects effectively. And the new method aims to improve the efficiency of solving optimization. In the optimization, VBHFs in different stages are the design variables. The optimization objectives are wrinkling and tearing for the two are the most common defects in the complex outer shell thin-walled part. Set the estimation criteria corresponding to wrinkling and tearing. And the constrains are limiting the two estimation criteria under two safety thresholds. After established the optimization problem, the LHD is used for sampling. The Kriging surrogate model is adopted to express the optimization in mathematical form. Then the multi-objectives QO-Jaya algorithm is introduced in solving the optimization problem. A numerical example of the complex outer shell thin-walled part is conducted to verify the effectiveness of the method. We use TOPSIS to select the best solutions that each algorithm generates, and put them in Dynaform for simulation and visual comparison.

We adopt Jaya algorithm as solver for it without algorithm-specific parameters and only having common control parameters, which save solving times and ensure the universality of the algorithm. The improved

multi-objective QO-Jaya algorithm in this paper includes three parts of contribution. First, the concepts of constraint-dominance sorting, non-dominance sorting and crowding distance computation are used to determine the rank of solutions. Second, the strategy of opposition-based learning is used to generate a population opposite to the current population. It further diversifies the population and accelerates the convergence rate of Jaya algorithm. Thirdly, the measurement index '*spread*' is defined to reflect the solutions convergence objectively. A new stop criterion is raised based on the *spread*. The improved multi-objective QO-Jaya algorithm (improved QO-Jaya algorithm in short) is compared with the common Jaya algorithm, NSGA-II algorithm and so on. It verifies the good performance of improved QO-Jaya algorithm in solving optimization.

In future, we can study the VBHF coupling with other parameters in process optimization of deep drawing. Consider whether the parameters have uncertainty in optimization. The solving algorithm can be focused on how to balance the exploitation and exploration. We have considered the hybrid algorithm initially to improve the problem.

Acknowledgements
Not applicable.

Authors' Contributions
XJ was in charge of the modeling, data analysis and writing the manuscript; ZH reviewed and edited the manuscript. YF provided the data test platform, resources, and funding acquisition. JT was in charge of supervision and project administration. All authors read and approved the final manuscript.

Author's Information
Xiangyu Jiang, born in 1997, is currently a PhD candidate at *State Key Laboratory of Fluid Power and Mechatronic Systems, Zhejiang University, China*. Her research interests include intelligent operation and maintenance of equipment.
Zhaoxi Hong, born in 1990, is currently an assistant research fellow at *State Key Laboratory of Fluid Power and Mechatronic Systems, Zhejiang University, China*. Her research interests include low-carbon mechanical product design and uncertain optimization in intelligent manufacturing.
Yixiong Feng, born in 1975, is currently a professor and a PhD candidate supervisor at *State Key Laboratory of Fluid Power and Mechatronic Systems, Zhejiang University, China*. His main research interests include mechanical product design theory, intelligent automation, and advance manufacture technology.
Jianrong Tan, born in 1954, is currently an academician of *Chinese Academy of Engineering, China,* a specially appointed professor and a PhD candidate supervisor at *Zhejiang University*, *China*. His main research interests include mechanical design and theory, computer aided design and graphics, digital design and manufacturing.

Funding
Supported by National Key Research and Development Program of China (Grant No. 2022YFB3304200), National Natural Science Foundation of China (Grant No. 52075479), and Taizhou Municipal Science and Technology Project of China (Grant No.1801gy23).

Availability of data and materials
Not applicable.

Declarations

Competing Interests
The authors declare no competing financial interests.

Received: 29 September 2021 Revised: 24 July 2023 Accepted: 30 November 2023
Published online: 05 January 2024

References

[1] R Dwivedi, G Agnihotri. Study of deep drawing process parameters. *Materials Today: Proceedings*, 2017, 4: 820–826.
[2] S T Atul, M C L Babu. A review on effect of thinning, wrinkling and spring-back on deep drawing process. *Proceedings of the Institution of Mechanical Engineers, Part B: Journal of Engineering Manufacture*, 2019, 233: 1011–1036.
[3] L Zheng, Z Wang, Z Liu, et al. Formability and performance of 6K21-T4 aluminum automobile panels in VPF under variable blank holder force. *International Journal of Advanced Manufacturing Technology*, 2018, 94: 571–584.
[4] C Su, K Zhang, S Lou, et al. Effects of variable blank holder forces and a controllable drawbead on the springback of shallow-drawn TA2M titanium alloy boxes. *International Journal of Advanced Manufacturing Technology*, 2017, 93: 1627–1635.
[5] B Modi, D R Kumar. Development of a hydroforming setup for deep drawing of square cups with variable blank holding force technique. *International Journal of Advanced Manufacturing Technology*, 2013, 66: 1159–1169.
[6] J Srirat, S Kitayama, K Yamazaki. Optimization of initial blank shape with a variable blank holder force in deep-drawing via sequential approximate optimization. *Journal of Advanced Mechanical Design, Systems, and Manufacturing*, 2012, 6: 1093–1106.
[7] B Lela, J Krolo, T Mirić. Mathematical modelling of an experimental-analytical method for friction coefficient determination in deep drawing. *Materials Science and Engineering Technology*, 2019, 50: 372–381.
[8] D K Karupannasamy, J Hol, M B de Rooij, et al. Modelling mixed lubrication for deep drawing processes. *Wear*, 2012, 294–295: 296–304.
[9] F Gong, Z Yang, Q Chen, et al. Influences of lubrication conditions and blank holder force on micro deep drawing of C1100 micro conical–cylindrical cup. *Precision Engineering*, 2015, 42: 224–230.
[10] J Lin, Y Chen, S Chiou. Optimization of double-square-slot deep drawing process. *Steel Research International*, 2010, 81: 604–607.
[11] S Kitayama, H Koyama, K Kawamoto, et al. Numerical and experimental case study on simultaneous optimization of blank shape and variable blank holder force trajectory in deep drawing. *Structural and Multidisciplinary Optimization*, 2017, 55: 347–359.
[12] S Kitayama, S Huang, K Yamazaki. Optimization of variable blank holder force trajectory for springback reduction via sequential approximate optimization with radial basis function network. *Structural and Multidisciplinary Optimization*, 2013, 47: 289-–300.
[13] S Kitayama, S Hamano, K Yamazaki, et al. A closed-loop type algorithm for determination of variable blank holder force trajectory and its application to square cup deep drawing. *International Journal of Advanced Manufacturing Technology*, 2010, 51: 507–517.
[14] M A Ablat, A Qattawi. Numerical simulation of sheet metal forming: A review. *International Journal of Advanced Manufacturing Technology*, 2017, 89: 1235–1250.
[15] H Kim, S K Hong. FEM-based optimum design of multi-stage deep drawing process of molybdenum sheet. *Journal of Materials Processing Technology*, 2007, 184: 354–362.
[16] S K Singh, A Dixit, D R Kumar. Optimization of the design parameters of modified die in hydro-mechanical deep drawing using LS-DYNA. *International Journal of Advanced Manufacturing Technology*, 2008, 38(1–2): 32–37.
[17] M Manoochehri, F Kolahan. Integration of artificial neural network and simulated annealing algorithm to optimize deep drawing process.

International Journal of Advanced Manufacturing Technology, 2014, 73: 241–249.
[18] Y Tian, Y M Xie, X Q Sun, et al. Process parameters optimization of deep drawing based on fish RBF neural network and improved ant colony algorithm. *Forging and Stamping Technology*, 2014, 39: 129–136.
[19] Y Feng, R Lu, Y Gao, et al. Multi-objective optimization of VBHF in sheet metal deep-drawing using Kriging, MOABC, and set pair analysis. *International Journal of Advanced Manufacturing Technology*, 2018, 96: 3127–3138.
[20] Y Xie, Y Guo, F Zhang, et al. An efficient parallel infilling strategy and its application in sheet metal forming. *International Journal of Precision Engineering and Manufacturing*, 2020, 21: 1479–1490.
[21] S Kitayama, J Srirat, M Arakawa, et al. Sequential approximate multi-objective optimization using radial basis function network. *Structural and Multidisciplinary Optimization*, 2013, 48: 501–515.
[22] S Kitayama, H Yoshioka. Springback reduction with control of punch speed and blank holder force via sequential approximate optimization with radial basis function network. *International Journal of Mechanics and Materials in Design*, 2014, 10: 109–119.
[23] S Kitayama, M Saikyo, K Kawamoto, et al. Multi-objective optimization of blank shape for deep drawing with variable blank holder force via sequential approximate optimization. *Structural and Multidisciplinary Optimization*, 2015, 52: 1001–1012.
[24] M Lin, J Tsai, C Yu, et al. A review of deterministic optimization methods in engineering and management. *Mathematical Problems in Engineering*, 2012, 6: 183–190.
[25] E Li, H Wang. An alternative adaptive differential evolutionary algorithm assisted by expected improvement criterion and cut-HDMR expansion and its application in time-based sheet forming design. *Advances in Engineering Software*, 2016, 97: 96–107.
[26] Y Feng, Z Hong, Y Gao, et al. Optimization of variable blank holder force in deep drawing based on support vector regression model and trust region. *International Journal of Advanced Manufacturing Technology*, 2019, 105: 4265–4278.
[27] R V Rao. Jaya: A simple and new optimization algorithm for solving constrained and unconstrained optimization problems. *International Journal of Industrial Engineering Computations*, 2016, 7: 19–34.
[28] R V Rao, V J Savsani, D P Vakharia. Teaching–learning-based optimization: a novel method for constrained mechanical design optimization problems. *Computer-Aided Design*, 2011, 43: 303–315.
[29] L Zhao, P Wang, B Song, et al. An efficient kriging modeling method for high-dimensional design problems based on maximal information coefficient. *Structural and Multidisciplinary Optimization*, 2020, 61: 39–57.
[30] M D Mckay, R J Beckman, W J Conover. A comparison of three methods for selecting values of input variables in the analysis of output from a computer code. *Technometrics*, 2000, 42: 55–61.
[31] R V Rao, G G Waghmare. A new optimization algorithm for solving complex constrained design optimization problems. *Engineering Optimization*, 2017, 49: 60–83.
[32] Y Zhang, X Yang, C Cattani, et al. Tea category identification using a novel fractional fourier entropy and Jaya algorithm. *Entropy (Basel, Switzerland)*, 2016, 18: 77.
[33] R V Rao, D P Rai, J Balic. A multi-objective algorithm for optimization of modern machining processes. *Engineering Applications of Artificial Intelligence*, 2017, 61: 103–125.
[34] R V Rao, K C More. Design optimization and analysis of selected thermal devices using self-adaptive Jaya algorithm. *Energy Conversion and Management*, 2017, 140: 24–35.
[35] R V Rao, D P Rai. Optimization of submerged arc welding process parameters using quasi-oppositional based Jaya algorithm. *Journal of Mechanical Science and Technology*, 2017, 31: 2513–2522.
[36] A Farah, A Belazi. A novel chaotic Jaya algorithm for unconstrained numerical optimization. *Nonlinear Dynamics*, 2018, 93: 1451–1480.
[37] K Yu, B Qu, C Yue, et al. A performance-guided JAYA algorithm for parameters identification of photovoltaic cell and module. *Applied Energy*, 2019, 237: 241–257.
[38] R V Rao, A Saroj. Constrained economic optimization of shell-and-tube heat exchangers using elitist-Jaya algorithm. *Energy*, 2017, 128: 785–800.